# Diagnosis and Tolerant Strategy of an Open-Switch Fault for T-Type Three-Level Inverter Systems

Ui-Min Choi, *Student Member, IEEE*, Kyo-Beum Lee, *Senior Member, IEEE*, and Frede Blaabjerg, *Fellow, IEEE*

***Abstract*—This paper proposes a new diagnosis method of an open-switch fault and fault-tolerant control strategy for T-type three-level inverter systems. The location of the faulty switch can be identified by the average of the normalized phase current and the change of the neutral-point voltage. The proposed fault-tolerant strategy is explained by dividing into two cases: the faulty condition of half-bridge switches and neutral-point switches. The performance of the T-type inverter system improves considerably by the proposed fault-tolerant algorithm when a switch fails. The proposed method does not require additional components and complex calculations. Simulation and experimental results verify the feasibility of the proposed fault diagnosis and fault-tolerant control strategy.**

***Index Terms*—Fault tolerance, multilevel, open-switch fault, reliability, T-type inverter.**

## I. Introduction

RECENTLY, the three-level T-type inverter has been proposed for high-efficiency systems in low-voltage applications such as photovoltaic (PV) inverter, power factor corrector (PFC) rectifier, and automotive inverter systems [1]. Fig. 1 shows the simplified circuit of a T-type inverter. The T-type inverter uses the same switch as that used in a conventional two-level inverter because these switches ($S_{x1(x=a,b,c)}$ and $S_{x4}$) have to block the full dc-link voltage. A bidirectional switch is connected between the neutral point and each output. Unlike the half-bridge switches ($S_{x1}$ and $S_{x4}$), the bidirectional switches ($S_{x2}$ and $S_{x3}$) have to block only half of the dc-link voltage. Therefore, it is possible to use the devices having a lower voltage rating. The neutral-point clamped (NPC) inverter uses the two switches connected in series to block the full dc-link voltage. On the other hand, the T-type inverter uses a single switch to block the full dc-link voltage. Therefore, the conduction losses of the T-type inverter are considerably reduced compared to that of the NPC inverter. The T-type inverter has reduced switching losses and switching noise because the neutral-point switches are operated under the half of the dc-link voltage. Therefore, the total losses in a T-type inverter are the lowest among those of the two-level, NPC, and T-type inverters in medium switching frequencies (4–30 kHz) [1]–[4].

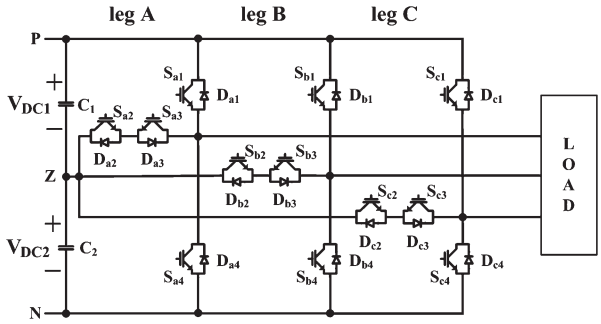


Fig. 1. Simplified structure of the T-type inverter systems.

Nowadays, the interest in the reliability has been increasing because it is closely related to the cost and efficiency of the overall systems. Therefore, many research works about the reliability of power conversion systems are conducted, particularly for the fault detection and fault-tolerant control of the switching device [5]–[9]. The switching device fault can be classified as a short-switch fault and an open-switch fault [10]. A short-switch fault can occur because of the several reasons such as the wrong gate voltage, overvoltage, avalanche stress, or too high temperature. A short-switch fault is difficult to handle because an abnormal overcurrent which can cause serious damage to other parts is produced immediately if the short-switch fault occurs. Therefore, most methods of short-switch fault detection and tolerant control are based on hardware circuits [10]–[13]. An open-switch fault occurs due to the lifting of bonding wire caused by the thermal cycling. Open-switch faults lead to current distortion and can cause secondary problems in other components such as gate drivers and other insulated gate bipolar transistors (IGBTs) through induced noise and vibrations. An open-switch fault does not typically generate serious damage, compared to short-circuit faults, but does reduce the system performance. Therefore, detection methods of open-switch faults and fault-tolerant control are needed in power electronic systems [10]–[13].

Several researchers introduced fault-tolerant strategies for the well-known topologies such as an NPC inverter [14], [15], a flying capacitor inverter [16], an H-bridge multilevel inverter [17], [18], etc. In [14] and [15], the additional fourth leg replaces the faulty leg when the fault occurs. In [16], using the additional switch components, the faulty switch is bypassed or force closed. Then, it changes the modulation method for

Manuscript received November 12, 2012; revised April 14, 2013; accepted May 5, 2013. Date of publication June 18, 2013; date of current version January 16, 2014. Paper 2012-IPCC-583.R1, presented at the 2012 IEEE Energy Conversion Congress and Exposition, Raleigh, NC, USA, September 15–20, and approved for publication in the IEEE TRANSACTIONS ON INDUSTRY APPLICATIONS by the Industrial Power Converter Committee of the IEEE Industry Applications Society. This work was supported by the Basic Science Research Program through the National Research Foundation of Korea funded by the Ministry of Education (2013R1A1A2A10006090).

U.-M. Choi and F. Blaabjerg are with the Department of Energy Technology, Aalborg University, 9220 Aalborg East, Denmark (e-mail: uch@et.aau.dk; fbl@et.aau.dk).

K.-B. Lee is with the Department of Electrical and Computer Engineering, Ajou University, Suwon 443-749, Korea, and also with San5, Suwon 443-749, Korea (e-mail: kyl@ajou.ac.kr).

Color versions of one or more of the figures in this paper are available online at http://ieeexplore.ieee.org.

Digital Object Identifier 10.1109/TIA.2013.2269531

fault-tolerant control. The methods proposed in [17] and [18] also bypass the faulty converter using the additional components and change the modulation method which does not use the faulty converter. All of these methods require additional components for continuous operation such as IGBTs, diodes, thyristors, fuses, etc. These are not cost-effective. Furthermore, the existing methods are specialized in each topology. Hence, it is difficult to directly use the existing methods to T-type three-level inverter systems.

This paper analyzes the operation of the T-type three-level inverter under open-switch fault conditions and presents fault diagnosis methods and also tolerant control strategies. The faulty switch can be identified by the average of the normalized phase current and the change of the neutral-point voltage. The proposed fault-tolerant strategy is explained by dividing into two cases: when the open-switch fault occurs in half-bridge switches ($S_{x1}$ and $S_{x4}$) and in neutral-point switches ($S_{x2}$ and $S_{x3}$). The proposed method can improve the reliability of the small power systems such as PV inverter systems, PFC rectifiers, and electric machine drive systems. The simulation and experimental results confirm the feasibility and reliability of the proposed methods.

## II. Analysis of T-Type Three-Level Inverter During Open-Switch Fault

If an open-switch fault occurs, the current path is different with the current path under normal conditions because the switching states do not reach the desired states. It produces the undesirable output pole voltages and causes the distortion of output phase currents and change of neutral-point voltage. The analysis is implemented considering only one switch fault because it is rare that the open-switch fault occurs in more than one switch at the same time.

### A. Change of Phase Currents and Output Pole Voltage

Figs. 2–5 show the current path and the output pole voltage under normal and fault conditions, respectively. The solid line indicates the current path under normal conditions, and the dashed line denotes the current path under fault conditions. The positive current direction is defined as flowing out from the inverter to the loads. Under normal conditions, if the switching state is [P] and the phase current $I_a > 0$, the phase current flows through the switch $S_{a1}$, and the pole voltage becomes $+V_{\rm DC}/2$.

However, if the open fault occurs in switch $S_{a1}$, the current flows through the switch $S_{a2}$ and the diode $D_{a3}$, and the phase output are connected to the neutral point instead of the positive dc bus as shown in Fig. 2(a). If the phase current $I_a < 0$ during the switching state is [P], the current flows through the diode $D_{a1}$ in both cases as shown in Fig. 2(b). Therefore, there are no distortion in the pole voltage and the phase current.

In the case of the switch $S_{a2}$ fault, if the switching state is [O] and the phase current $I_a > 0$, the current flows through the diode $D_{a4}$ instead of the switch $S_{a2}$ and the diode $D_{a3}$. The pole voltage becomes $-V_{\rm DC}/2$ because the phase output is connected to the negative dc bus as shown in Fig. 3(a). It causes a distortion of phase current. Fig. 3(b) shows the current paths when the phase current $I_a < 0$. Under normal conditions, the current flows through the switch $S_{a3}$ and the diode $D_{a2}$. The current path under the switch $S_{a2}$ fault condition is the same with the current path under normal conditions.

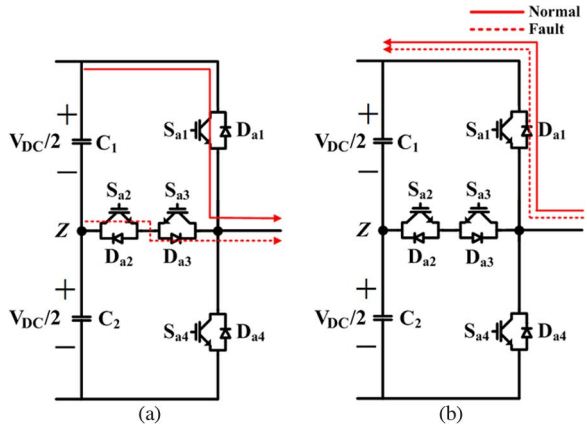


Fig. 2. Current path under normal and switch $S_{a1}$ fault conditions. (a) $I_a > 0$. (b) $I_a < 0$.

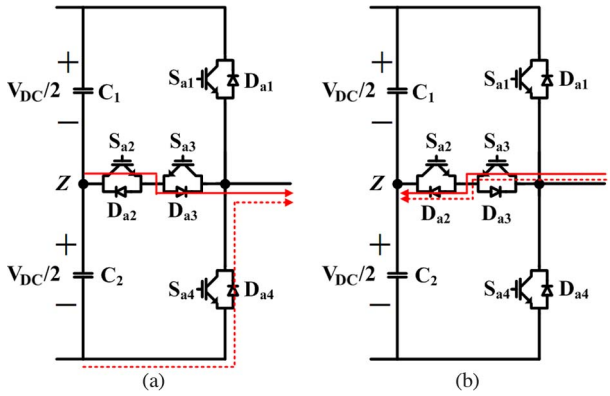


Fig. 3. Current path under normal and switch $S_{a2}$ fault conditions. (a) $I_a > 0$. (b) $I_a < 0$.

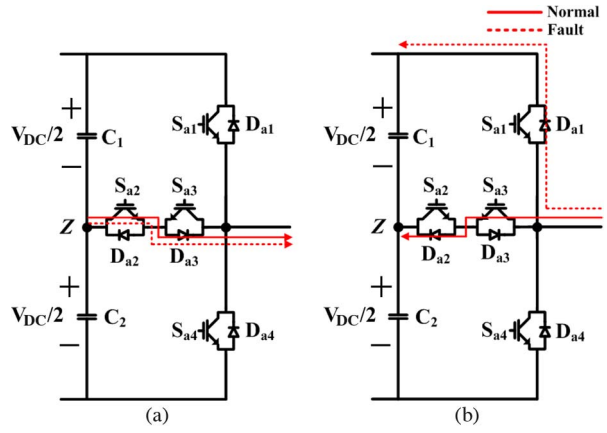


Fig. 4. Current path under normal and switch $S_{a3}$ fault conditions. (a) $I_a > 0$. (b) $I_a < 0$.

If the switching state is [O] and the phase current $I_a > 0$, the current flows through the switch $S_{a2}$ and the diode $D_{a3}$ under normal and switch $S_{a3}$ fault conditions as shown in Fig. 4(a). Fig. 4(b) shows the current paths when the phase current $I_a < 0$. Under normal conditions, the current flows

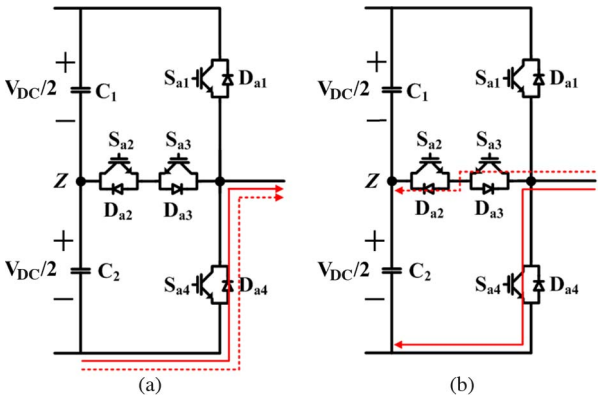


Fig. 5. Current path under normal and switch $S_{a4}$ fault conditions. (a) $I_a > 0$. (b) $I_a < 0$.

through the switch $S_{a3}$ and diode $D_{a2}$. However, under the switch $S_{a3}$ fault condition, the current flows through the diode $D_{a1}$, and the phase output is connected to the positive dc bus rather than the neutral point.

As shown in Fig. 5(a), if the current $I_a > 0$ and the switching state is [N], the current path is formed through the diode $D_{a4}$ regardless of the switch $S_{a4}$ fault. If the current $I_a < 0$ during the switching state [N], the current flows through the switch $S_{a4}$ under normal conditions; however, if an open fault occurs in switch $S_{a4}$, the current flows through switch $S_{a3}$ and diode $D_{a2}$, and the phase voltage becomes zero rather than $-V_{\rm DC}/2$ as shown in Fig. 5(b). Because of an open-switch fault, the undesirable output pole voltage is produced, and the phase current is distorted. It causes an unbalance of neutral-point voltage.

### *B. Change of Neutral-Point Voltage*

The neutral-point voltage is analyzed under the assumption that the T-type inverter is in normal operation (inverter mode) and the open-switch fault occurs in leg A [19], [20].

If the open-switch fault occur at the switch $S_{x1}$, the switching state [P] is impossible. Supposing that the open-switch fault occurs in the switch $S_{a1}$ of leg A and the inverter is in normal operation, the switching states of P-type small voltage vectors [PPO], [POO], and [POP], the switching states of medium vectors [PON] and [PNO], and the switching states of large voltage vectors [PNN], [PPN], and [PNP] are impossible. These vectors are replaced with the switching state to themselves which includes state [O] in the faulty leg A. For example, the switching state [PNN] is replaced with the switching state [ONN]. On the contrary, the other switching states which contain the switching state [O] or [N] in the faulty leg A are possible. Therefore, the upper capacitor voltage $V_{\rm DC1}$ becomes larger than the lower capacitor voltage $V_{\rm DC2}$.

When the open-switch fault occurs in switch $S_{x2}$, the switching state [O] is impossible, and this state is replaced with the switching state [N]. In the faulty leg A case, the switching states [ONN], [OON], [ONO], [OPN], and [ONP] are impossible. These switching states are also changed to the switching states which includes not the [O] state but the [N] state in the faulty leg A. The amount of neutral current flowing out from the neutral point is smaller than that under the normal condition. Therefore, the lower capacitor voltage $V_{\rm DC2}$ is larger than the upper capacitor voltage $V_{\rm DC1}$.

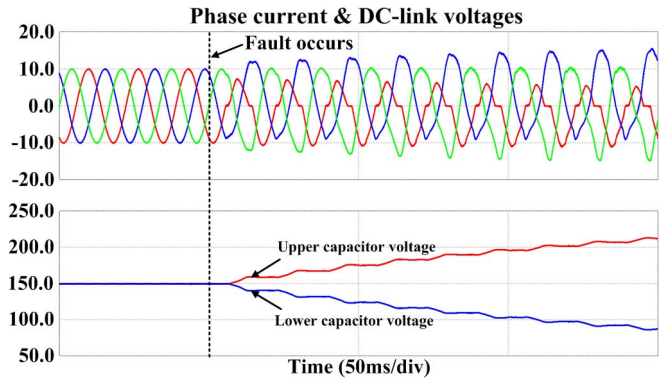


Fig. 6. Phase current and dc-link voltages when an open fault occurs in switch $S_{a1}$.

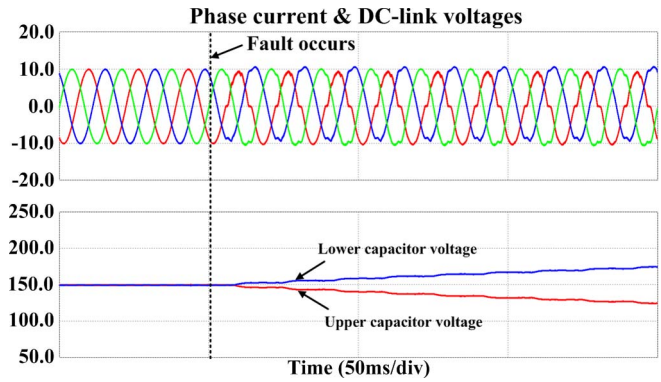


Fig. 7. Phase current and dc-link voltages when an open fault occurs in switch $S_{a2}$.

The overall analysis with regard to the open-switch fault in switch $S_{x3}$ is similar to that in switch $S_{x2}$ except the current direction. In this case, the switch state [O] is impossible, and it is replaced with the switching state [P] in the faulty leg. Contrary to the upper case, the amount of neutral current flowing into the neutral point is smaller than that under the normal condition. Therefore, the upper capacitor voltage $V_{\rm DC1}$ is bigger than the lower capacitor voltage $V_{\rm DC2}$.

If the open switch occurs in switch $S_{x4}$, the switching state [N] is replaced with the state [O]. In case of the faulty leg A, the switching states [NON], [NOO], [NNO], [NPO], [NOP], [NPN], [NPP], and [NNP] are impossible, and these states are replaced by the switching states which contain the switching state [O] instead of [N] in the faulty leg A. In this case, the amount of phase current flowing into the neutral point is larger than the amount of phase current flowing out from the neutral point. Therefore, the lower capacitor voltage $V_{\rm DC2}$ is bigger than the upper capacitor voltage $V_{\rm DC1}$.

Figs. 6–9 show the simulated phase currents and neutral-point voltage according to the faulty switch, respectively.

## III. Diagnosis Method of an Open-Switch Fault

If the open-switch fault occurs, the phase current is distorted, and the neutral-point voltage is unbalanced as shown in the

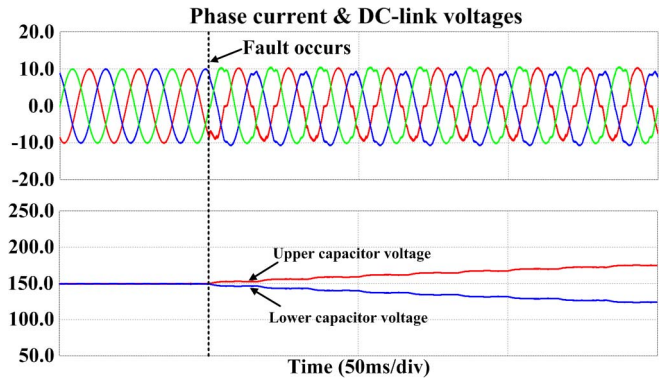


Fig. 8. Phase current and dc-link voltages when an open fault occurs in switch $S_{a3}$.

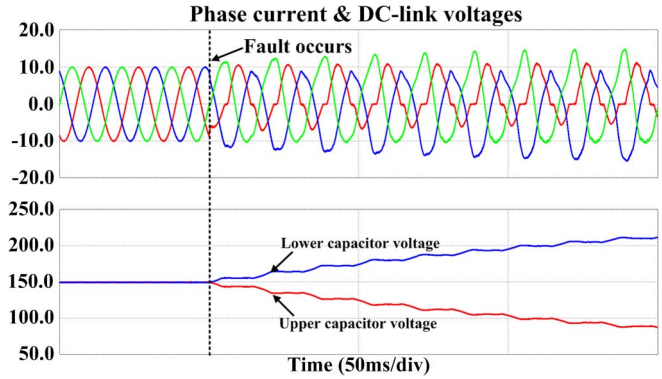


Fig. 9. Phase current and dc-link voltages when an open fault occurs in switch $S_{a4}$.

previous analysis. Using these values, the faulty switch can be identified [8], [9].

Under the normal condition, the average of the phase current is zero. However, in the faulty cases, the value of the phase current's average is changed. If the open-switch fault occurs in the switch $S_{x1}$ or switch $S_{x2}$, the average of the phase current is a negative value because the positive phase current is distorted. If the open-switch fault occurs in the switch $S_{x3}$ or switch $S_{x4}$, the average of the phase current has a positive value because the negative phase current is distorted in the faulty leg. The averages of the other phase currents are also changed due to the distortion of the phase current in the faulty leg. However, if these values are used directly, these values may lead to false alarm when harmonic components exist in the phase current or when this system is notably under fast transients. To improve the accuracy of detection, the normalized current method is employed. The normalized current can be obtained through the following equation:

$$|\bar{I}_s| = |I_{ds}| + |I_{qs}| = \sqrt{(I_{ds})^2 + (I_{qs})^2} \tag{1}$$

$$I_{xN} = \frac{I_x}{|\bar{I}_s|} \times K \tag{2}$$

where $x = a, b, c$, $I_{ds}$ and $I_{qs}$ are the reactive and the active current of the stationary reference frame, respectively, and $K$ is the magnitude of the normalized phase current.

TABLE I
VALUES OF DIAGNOSIS VARIABLES

| | Diagnosis Variables | | | |
|---|---|---|---|---|
| Fault Switch | $\mu_a$ | $\mu_b$ | $\mu_c$ | $V_d$ |
| $S_{a1}$ | -1 | +1 | – | +1 |
| $S_{a2}$ | -1 | +1 | – | -1 |
| $S_{a3}$ | +1 | -1 | – | +1 |
| $S_{a4}$ | +1 | -1 | – | -1 |
| $S_{b1}$ | – | -1 | +1 | +1 |
| $S_{b2}$ | – | -1 | +1 | -1 |
| $S_{b3}$ | – | +1 | -1 | +1 |
| $S_{b4}$ | – | +1 | -1 | -1 |
| $S_{c1}$ | +1 | – | -1 | +1 |
| $S_{c2}$ | +1 | – | -1 | -1 |
| $S_{c3}$ | -1 | – | +1 | +1 |
| $S_{c4}$ | -1 | – | +1 | -1 |

– : unconcerned case

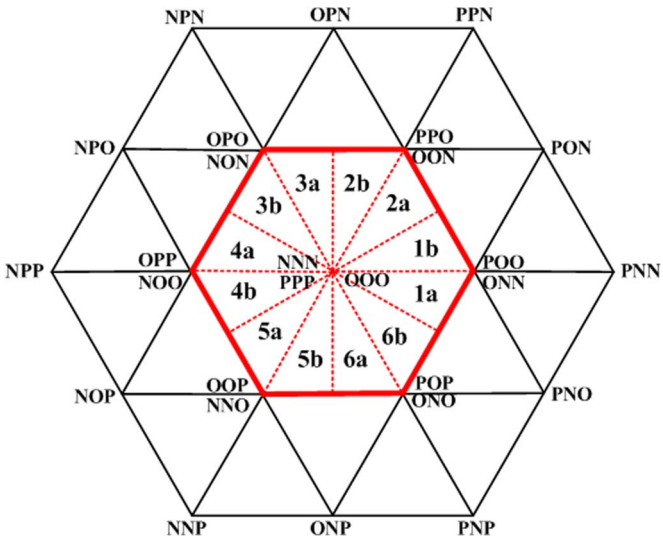


Fig. 10. Space vector diagram for fault-tolerant control when the open-switch fault occurs in half-bridge switches ($S_{x1}$ and $S_{x4}$).

Using the change of two capacitor voltages, the faulty switch can be identified between the switch $S_{x1}$ and switch $S_{x2}$ or between the switch $S_{x3}$ and switch $S_{x4}$. If $V_{\mathrm{DC1}}$ is bigger than the $V_{\mathrm{DC2}}$, the open-switch fault occurs in the switch $S_{x1}$ or switch $S_{x3}$. Reversely, if the $V_{\mathrm{DC2}}$ is larger than the $V_{\mathrm{DC1}}$, the open-switch fault occurs in switch $S_{x2}$ or switch $S_{x4}$. The procedure for the proposed fault diagnosis method is as follows.

1) Calculate the average of the normalized phase currents.
2) Using these values, identify the faulty leg and whether the open-switch faults occur in one of the two switches $S_{x1}$ and $S_{x2}$ or one of the two switches $S_{x3}$ and $S_{x4}$.
3) Identify the location of the faulty switch between $S_{x1}$ and $S_{x2}$ or between $S_{x3}$ and $S_{x4}$ using the change of two capacitor voltages.

To improve the accuracy, the threshold values $I_{thr}$ and $V_{thr}$ are set. The diagnosis variables $\mu_x$ and $V_d$ are defined by the

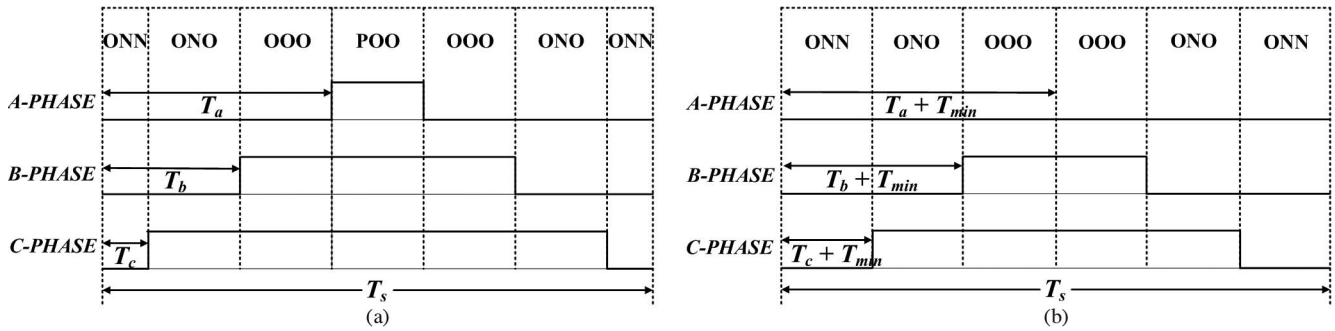


Fig. 11. Switching sequence when the reference voltage is in the region 1a. (a) Before $T_{\min}$ is added. (b) After $T_{\min}$ is added.

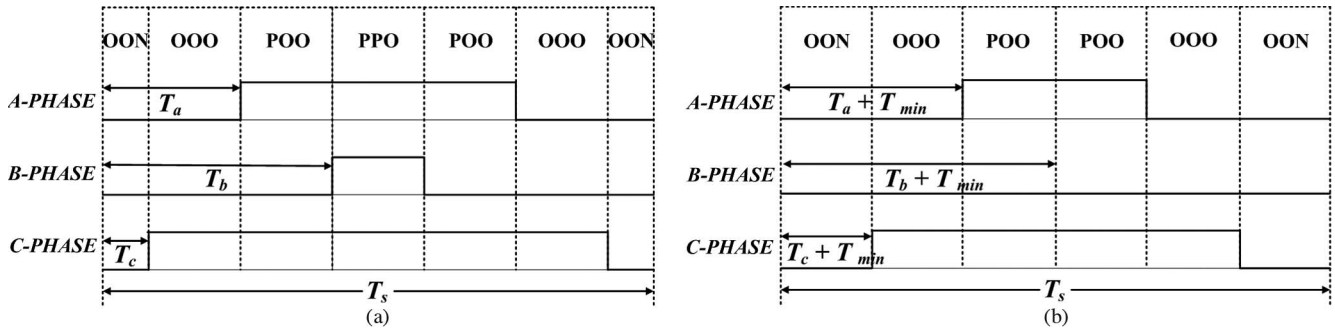


Fig. 12. Switching sequence when the reference voltage is in region 2a. (a) Before $T_{\min}$ is added. (b) After $T_{\min}$ is added.

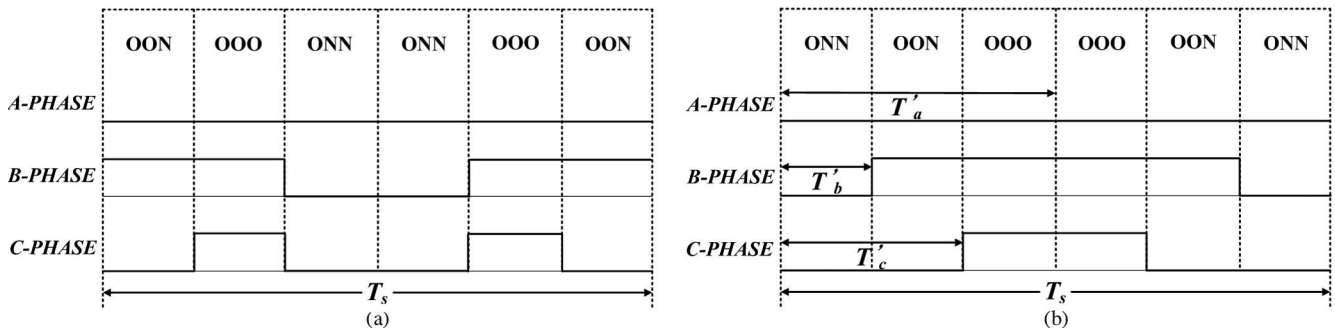


Fig. 13. Switching sequence when the reference voltage is in region 2a. (a) When the P-type switching state [POO] is replaced with N-type switching state [OON]. (b) When the switching sequence is rearranged.

following conditions:

$$\begin{aligned} &I_{xN\_avg} > I_{thr} && : \mu_x = 1 \\ &I_{xN\_avg} < -I_{thr} && : \mu_x = -1 \\ &-I_{thr} < I_{xN\_avg} < I_{thr} && : \mu_x = 0 \end{aligned}$$

$$\begin{aligned} &V_{\mathrm{DC1}} - V_{\mathrm{DC2}} > V_{thr} && : V_d = 1 \\ &V_{\mathrm{DC1}} - V_{\mathrm{DC2}} < -V_{thr} && : V_d = -1 \\ &-V_{th} < V_{\mathrm{DC1}} - V_{\mathrm{DC2}} < V_{thr} && : V_d = 0. \end{aligned} \quad (3)$$

Table I shows the diagnosis variables for the diagnosis of the open-switch fault.

## IV. Proposed Fault-Tolerant Control Strategy

The proposed fault-tolerant control strategy can be explained by dividing into two cases: the open-switch fault occurring in half-bridge switches ($S_{x1}$ and $S_{x4}$) and neutral-point switches ($S_{x2}$ and $S_{x3}$).

### A. Fault Occurring in Half-Bridge Switches ($S_{x1}$ and $S_{x4}$)

If the open-switch fault occurs in the half-bridge switches $S_{x1}$ and $S_{x4}$, the switching states [P] and [N] are impossible, respectively. Hence, the output phase current is distorted due to the undesirable output pole voltage as mentioned earlier.

In this case, the fault-tolerant strategy is proposed by being implemented as follows.

1) Reduce the modulation index so that the reference voltage is in the inner hexagon as shown in Fig. 10.
2) If the open-switch fault occurs in the switch $S_{x1}$, add the minimum turn-on time $T_{\min}$ to the three phase turn-on times $(T_a, T_b, T_c)$ when the reference voltage is in the regions where the faulty leg contains the switching state [P].
3) If the open-switch fault occurs in the switch $S_{x4}$, subtract the minimum turn-on time $T_{\min}$ from the three phase turn-on times $(T_a, T_b, T_c)$ when the reference voltage is in the regions where the faulty leg contains the switching state [N].

TABLE II
REDEFINED THREE PHASE TURN-ON TIMES FOR FAULT-TOLERANT CONTROL

| | Faulty switch | | |
|---|---|---|---|
| Region | leg A ($S_{a1}$, $S_{a4}$) | leg B ($S_{b1}$, $S_{b4}$) | leg C ($S_{c1}$, $S_{c4}$) |
| 1a | $T_a^{'} = T_a + T_{min}$<br>$T_b^{'} = T_b + T_{min}$<br>$T_c^{'} = T_c + T_{min}$ | $T_a^{'} = T_a - T_b$<br>$T_b^{'} = T_s/2$<br>$T_c^{'} = T_s/2 + T_c - T_b$ | $T_a^{'} = T_a - T_{min}$<br>$T_b^{'} = T_b - T_{min}$<br>$T_c^{'} = T_c - T_{min}$ |
| 1b | $T_a^{'} = T_a + T_{min}$<br>$T_b^{'} = T_b + T_{min}$<br>$T_c^{'} = T_c + T_{min}$ | $T_a^{'} = T_a - T_{min}$<br>$T_b^{'} = T_b - T_{min}$<br>$T_c^{'} = T_c - T_{min}$ | $T_a^{'} = T_a - T_c$<br>$T_b^{'} = T_s/2 + T_b - T_c$<br>$T_c^{'} = T_s/2$ |
| 2a | $T_a^{'} = T_s/2$<br>$T_b^{'} = T_b - T_a$<br>$T_c^{'} = 2T_c + T_b - T_a$ | $T_a^{'} = T_a + T_{min}$<br>$T_b^{'} = T_b + T_{min}$<br>$T_c^{'} = T_c + T_{min}$ | $T_a^{'} = T_a - T_{min}$<br>$T_b^{'} = T_b - T_{min}$<br>$T_c^{'} = T_c - T_{min}$ |
| 2b | $T_a^{'} = T_a + T_{min}$<br>$T_b^{'} = T_b + T_{min}$<br>$T_c^{'} = T_c + T_{min}$ | $T_a^{'} = T_a - T_b$<br>$T_b^{'} = T_s/2$<br>$T_c^{'} = +2T_c + T_a - T_b$ | $T_a^{'} = T_a - T_{min}$<br>$T_b^{'} = T_b - T_{min}$<br>$T_c^{'} = T_c - T_{min}$ |
| 3a | $T_a^{'} = T_a - T_{min}$<br>$T_b^{'} = T_b - T_{min}$<br>$T_c^{'} = T_c - T_{min}$ | $T_a^{'} = T_a + T_{min}$<br>$T_b^{'} = T_b + T_{min}$<br>$T_c^{'} = T_c + T_{min}$ | $T_a^{'} = T_s/2 + T_a - T_c$<br>$T_b^{'} = T_b - T_c$<br>$T_c^{'} = T_s/2$ |
| 3b | $T_a^{'} = T_s/2$<br>$T_b^{'} = T_b - T_a$<br>$T_c^{'} = T_s/2 - T_a + T_c$ | $T_a^{'} = T_a + T_{min}$<br>$T_b^{'} = T_b + T_{min}$<br>$T_c^{'} = T_c + T_{min}$ | $T_a^{'} = T_a - T_{min}$<br>$T_b^{'} = T_b - T_{min}$<br>$T_c^{'} = T_c - T_{min}$ |
| 4a | $T_a^{'} = T_a - T_{min}$<br>$T_b^{'} = T_b - T_{min}$<br>$T_c^{'} = T_c - T_{min}$ | $T_a^{'} = 2T_a + T_c - T_b$<br>$T_b^{'} = T_s/2$<br>$T_c^{'} = T_c - T_b$ | $T_a^{'} = T_a + T_{min}$<br>$T_b^{'} = T_b + T_{min}$<br>$T_c^{'} = T_c + T_{min}$ |
| 4b | $T_a^{'} = T_a - T_{min}$<br>$T_b^{'} = T_b - T_{min}$<br>$T_c^{'} = T_c - T_{min}$ | $T_a^{'} = T_a + T_{min}$<br>$T_b^{'} = T_b + T_{min}$<br>$T_c^{'} = T_c + T_{min}$ | $T_a^{'} = 2T_a + T_b - T_c$<br>$T_b^{'} = T_b - T_c$<br>$T_c^{'} = T_s/2$ |
| 5a | $T_a^{'} = T_s/2$<br>$T_b^{'} = T_s/2 + T_b - T_a$<br>$T_c^{'} = T_c - T_a$ | $T_a^{'} = T_a - T_{min}$<br>$T_b^{'} = T_b - T_{min}$<br>$T_c^{'} = T_c - T_{min}$ | $T_a^{'} = T_a + T_{min}$<br>$T_b^{'} = T_b + T_{min}$<br>$T_c^{'} = T_c + T_{min}$ |
| 5b | $T_a^{'} = T_a - T_{min}$<br>$T_b^{'} = T_b - T_{min}$<br>$T_c^{'} = T_c - T_{min}$ | $T_a^{'} = T_s/2 + T_a - T_b$<br>$T_b^{'} = T_s/2$<br>$T_c^{'} = T_c - T_b$ | $T_a^{'} = T_a + T_{min}$<br>$T_b^{'} = T_b + T_{min}$<br>$T_c^{'} = T_c + T_{min}$ |
| 6a | $T_a^{'} = T_a + T_{min}$<br>$T_b^{'} = T_b + T_{min}$<br>$T_c^{'} = T_c + T_{min}$ | $T_a^{'} = T_a - T_{min}$<br>$T_b^{'} = T_b - T_{min}$<br>$T_c^{'} = T_c - T_{min}$ | $T_a^{'} = T_a - T_c$<br>$T_b^{'} = 2T_b + T_a - T_c$<br>$T_c^{'} = T_s/2$ |
| 6b | $T_a^{'} = T_s/2$<br>$T_b^{'} = T_c + 2T_b - T_a$<br>$T_c^{'} = T_c - T_a$ | $T_a^{'} = T_a - T_{min}$<br>$T_b^{'} = T_b - T_{min}$<br>$T_c^{'} = T_c - T_{min}$ | $T_a^{'} = T_a + T_{min}$<br>$T_b^{'} = T_b + T_{min}$<br>$T_c^{'} = T_c + T_{min}$ |

4) When the switch $S_{x1}$ fails, if the P-type switching state of small vectors which has the switching state [P] on the faulty leg remained in regions where the $T_{\min}$ is added, replace this P-type switching state to the N-type switching state which indicates the same small voltage vector.
5) When the switch $S_{x4}$ fails, if the switching state of small vectors remained on the faulty leg which has the switching state [N], replace this N-type switching state to the P-type switching state which indicates the same small voltage vector.
6) To balance the neutral-point voltage, when the switch $S_{x1}$ fails, subtract the minimum turn-on time $T_{\min}$ when the reference voltage is in other regions where the faulty leg does not contain the switching state [P].
7) When the switch $S_{x4}$ fails, add the minimum turn-on time $T_{\min}$ when the reference voltage is in other regions

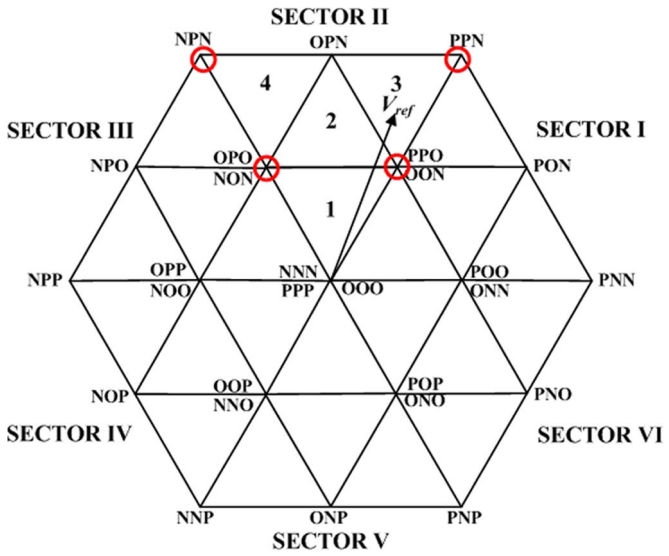


Fig. 14. Space vector diagram for fault-tolerant control when the open-switch fault occurs in neutral switches ($S_{x2}$ and $S_{x3}$).

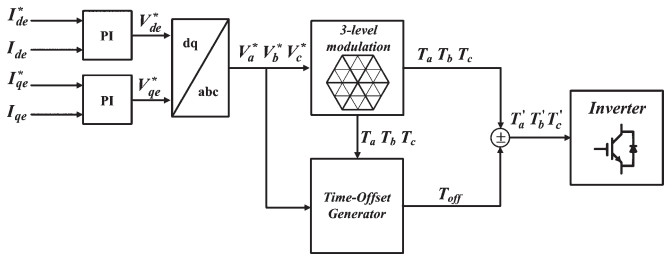


Fig. 15. Block diagram of proposed method when the open-switch fault occurs in neutral switches ($S_{x2}$ or $S_{x3}$).

TABLE III
PARAMETERS OF THE SIMULATIONS

| Parameter | Value |
|---|---|
| DC-link voltage | *300 V* |
| Switching frequency | *10 kHz* |
| Control period | *100 μs* |
| Frequency of current | *60 Hz* |
| Load | *L: 3mH, R: 15Ω* |
| $I_{th}$, $V_{th}$ | *0.08, 5V* |

where the faulty leg does not contain the switching state [N].

8) The N-type and P-type switching states' dwell time should be equal during the period of the reference voltage to balance the neutral-point voltage. In step 3, the P-type switching state is replaced with the N-type switching state when the open-switch fault occurs in $S_{x1}$. Therefore, among the remained N-type switching states in the regions where the $T_{\min}$ is subtracted, one of the N-type switching states should be replaced with the P-type switching state. At this step, the N-type switching state is chosen whose matched P-type switching state excludes the switching state [P] on the faulty leg, and this is when the switch $S_{x1}$ is faulty.
9) When the open-switch fault occurs in $S_{x4}$, the N-type switching state is substituted to the P-type switching state.

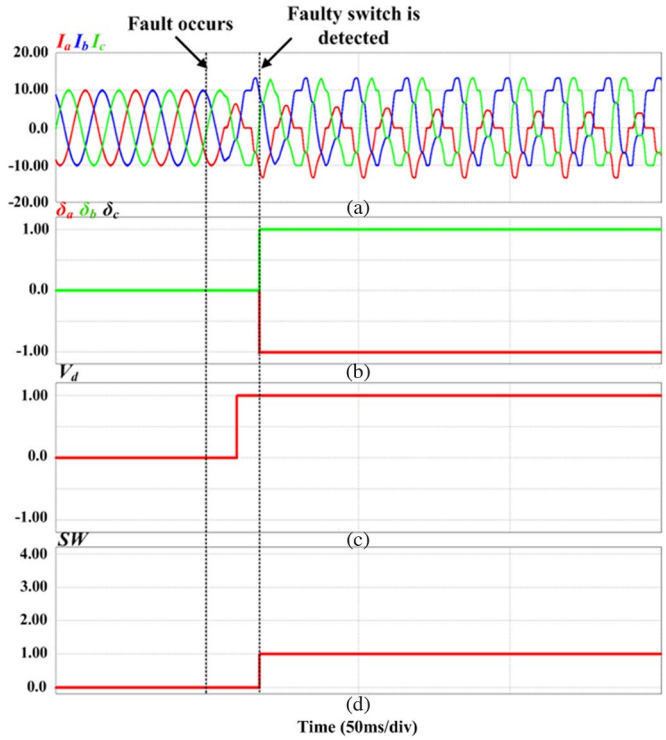


Fig. 16. Simulation results of proposed fault diagnosis method when switch $S_{a1}$ is faulty: (a) Phase currents, (b) diagnosis variables of average phase currents, (c) diagnosis variable of voltage difference, and (d) signal of faulty switch.

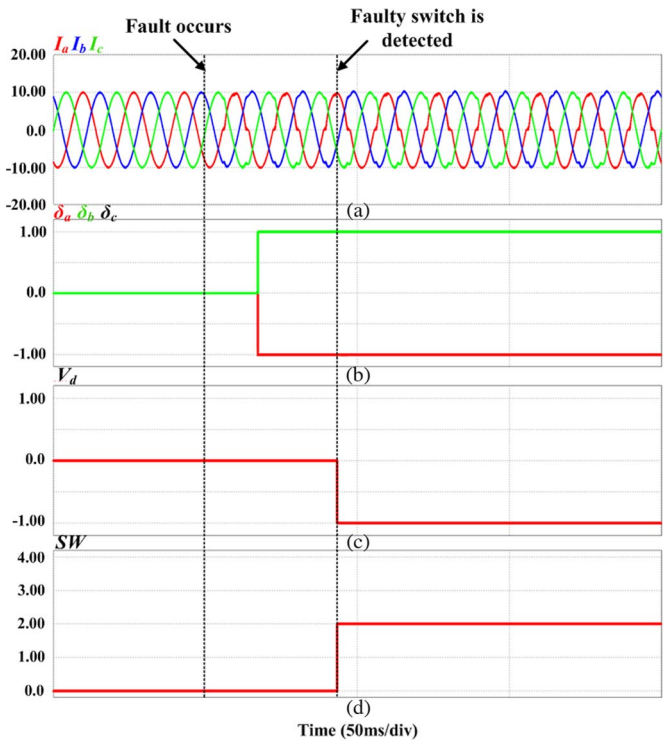


Fig. 17. Simulation results of proposed fault diagnosis method when switch $S_{a2}$ is faulty: (a) Phase currents, (b) diagnosis variables of average phase currents, (c) diagnosis variable of voltage difference, and (d) signal of faulty switch.

Hence, among the remained P-type switching states in the regions where the $T_{\min}$ is added, one P-type switching state has to be picked up. The required condition as the

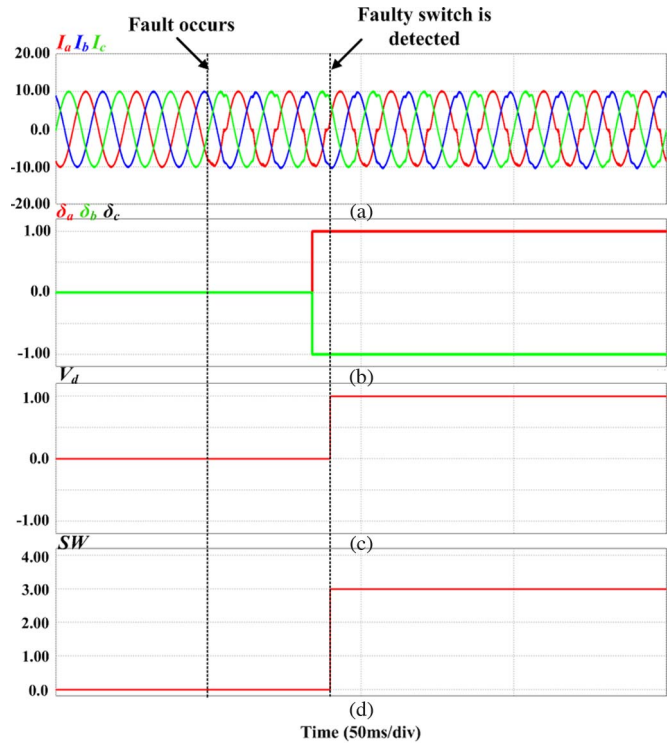


Fig. 18. Simulation results of proposed fault diagnosis method when switch $S_{a3}$ is faulty: (a) Phase currents, (b) diagnosis variables of average phase currents, (c) diagnosis variable of voltage difference, and (d) signal of faulty switch.

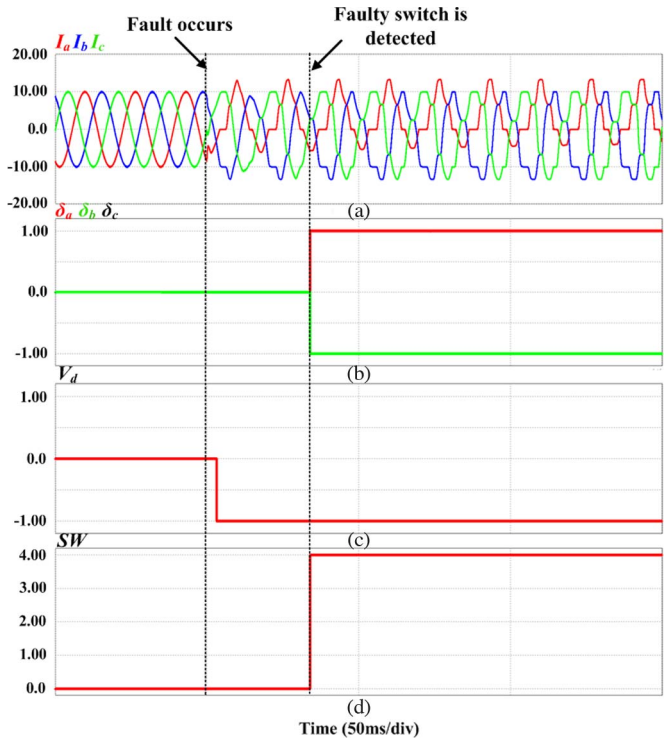


Fig. 19. Simulation results of proposed fault diagnosis method when switch $S_{a4}$ is faulty: (a) Phase currents, (b) diagnosis variables of average phase currents, (c) diagnosis variable of voltage difference, and (d) signal of faulty switch.

proper P-type switching state is that its matched N-type switching state does not contain the switching state [N] on a faulty leg.

10) Rearrange the switching sequence in order to reduce the number of switching.

To assist the understanding of the proposed method, the case of a leg A fault is considered.

If the open-switch fault occurs in the switch $S_{a1}$, reduce the modulation index so that the voltage reference is in the inner hexagon (red region). Then, add the $T_{\min}$ to the three phase turn-on times $(T_a, T_b, T_c)$ when the reference voltage is in the regions 1, 2, and 6.

Fig. 11 shows the switching sequence before the $T_{\min}$ is added and after the $T_{\min}$ is added when the voltage reference is in the region 1a. In this sequence, the $T_{\min}$ is $T_c$. As shown in Fig. 11(b), after the $T_{\min}$ is added, the new switching sequence is [OON]-[ONO]-[OOO]-[ONO]-[ONN]. In this sequence, the dwell time of the P-type switching state [POO] becomes zero, and the dwell time of the N-type switching state [ONN] is doubled in comparison with the conventional three-level space vector modulation (SVM). This does not affect the output phase voltage because the dwell times of the other switching states are unchanged and the small switching states [ONN] and [POO] generate the same line-to-line ac output voltage [21]. The distortion of the output does not occur because the faulty switch $S_{a1}$ is not used in this sequence.

However, in regions 2a and 6b, the P-type switching state [POO] still remained after the $T_{\min}$ is added as shown in Fig. 12. Therefore, the P-type switching state [POO] should be

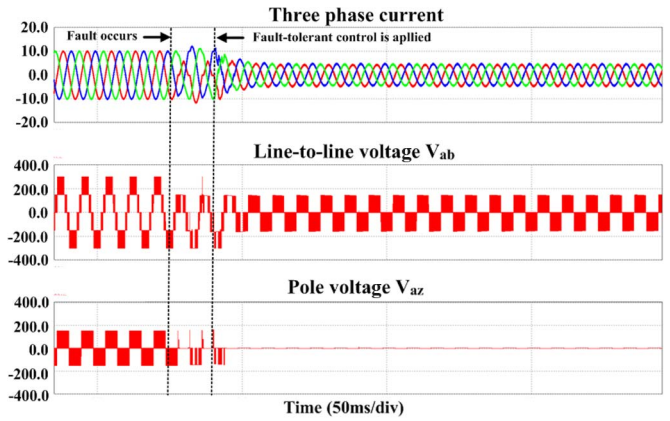


Fig. 20. Simulation results of proposed fault-tolerant control when the open-switch fault occurs in switch $S_{a1}$.

replaced with the N-type switching state [ONN] as shown in Fig. 13(a).

In regions 1, 2, and 6, the dwell time of the P-type switching state becomes zero, and the dwell time of the N-type switching state is doubled by adding the $T_{\min}$ to the three phase turn-on times. It causes an unbalance of the neutral-point voltage. To balance the neutral-point voltage, the $T_{\min}$ should be subtracted when the reference voltage is in regions 3, 4, and 5. Furthermore, the N-type switching state [NOO] should be replaced with the P-type switching state [OPP] in regions 3b and 5a. This is because the P-type switching state [POO] is substituted to [ONN] in regions 2a and 6b.

In regions 2a, 3b, 5a, and 6b, the number of switching is increased because the switching states of the small voltage vector are changed. Therefore, the switching sequence

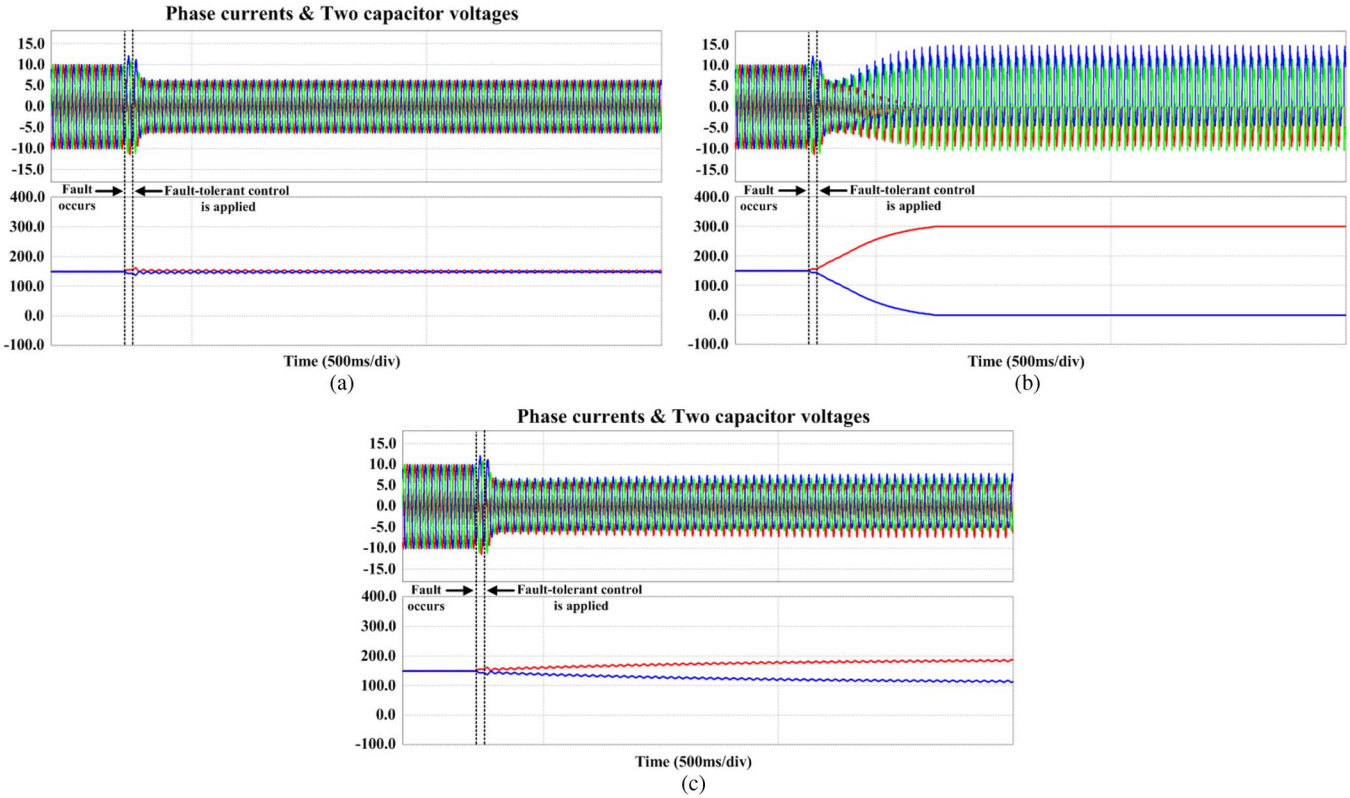


Fig. 21. Comparison results (a) when steps 3 and 4 are considered, (b) when steps 3 and 4 are not considered, and (c) when only step 4 is not considered.

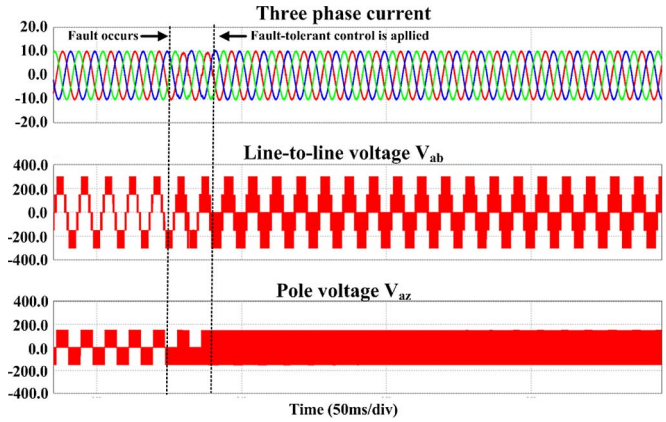


Fig. 22. Simulation results of the proposed fault-tolerant control when the open-switch fault occurs in switch $S_{a2}$.

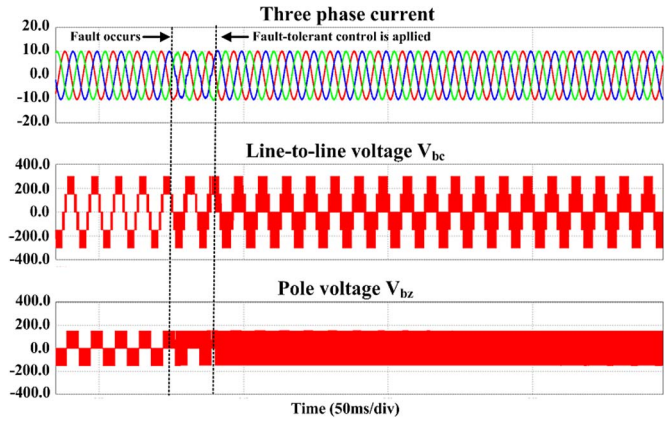


Fig. 23. Simulation results of the proposed fault-tolerant control when the open-switch fault occurs in switch $S_{b3}$.

should be rearranged in order to reduce the number of switching. For example, in region 2a, the switching sequence is [OON]-[OOO]-[ONN]-[OOO]-[OON] as shown in Fig. 13(a). In this switching sequence, leg c changes its switching state twice. To reduce the number of switching, the switching sequence should be rearranged as [ONN]-[OON]-[OOO]-[OON]-[ONN] as shown in Fig. 13(b). In order to rearrange the switching sequence as shown in Fig. 13(b), the dwell time of each switching state should be obtained. The dwell time can be expressed by the turn-on times as follows:

$$\begin{aligned} T_{dwell[\mathrm{OON}]} &= 2(T_c + T_{\min}) = 4T_c \\ T_{dwell[\mathrm{OOO}]} &= 2(T_a - T_c) \\ T_{dwell[\mathrm{POO}]} &= T_{dwell[\mathrm{ONN}]} = 2(T_b - T_a). \end{aligned} \tag{4}$$

Using these conditions, the three phase turn-on times $(T_a, T_b, T_c)$ are redefined as follows:

$$\begin{aligned} T_a^{'} &= T_s/2 \\ T_b^{'} &= \frac{1}{2} T_{dwell[\mathrm{ONN}]} = T_b - T_a \\ T_c^{'} &= \frac{1}{2}\left(T_{dwell[\mathrm{ONN}]} + T_{dwell[\mathrm{OON}]}\right) = 2T_c + T_b - T_a. \end{aligned} \tag{5}$$

Following the fault-tolerant strategy as explained earlier, the redefined turn-on times for tolerant control of the switch $S_{a4}$ fault are the same with the case of the switch $S_{a1}$ fault.

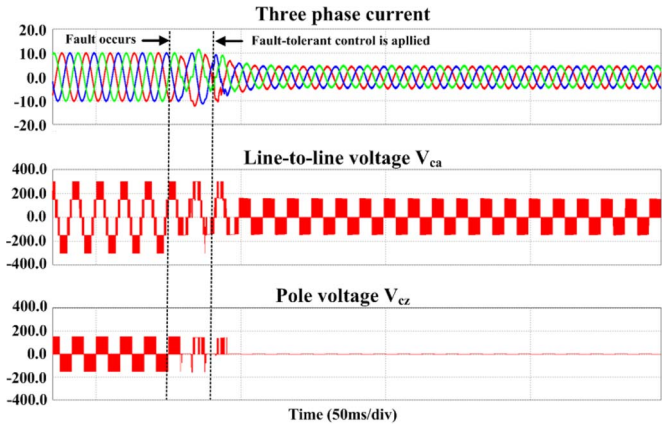


Fig. 24. Simulation results of the proposed fault-tolerant control when the open-switch fault occurs in switch $S_{c4}$.

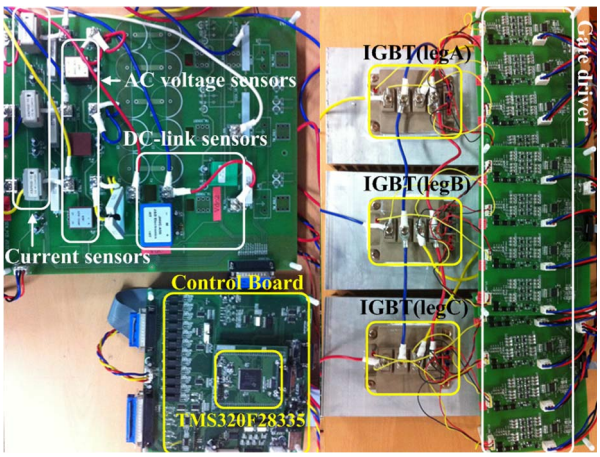


Fig. 25. Prototype of T-type three-level inverter systems.

The redefined turn-on times to achieve the fault-tolerant control are arranged in Table II.

### B. Fault Occurring in Neutral-Point Switches ($S_{x2}$ and $S_{x3}$)

If the open-switch fault occurs in $S_{x2}$, the output pole voltage is distorted when the current direction is positive because the pole voltage ($V_{xz}$) becomes $-V_{\rm DC}/2$ instead of zero while the switching state is [O]. On the contrary, if the open-switch fault occurs in $S_{x3}$, the output pole voltage becomes $+V_{\rm DC}/2$ instead of zero when the current direction is negative, while the switching state is [O]. The switching state [O] is impossible, but [P] and [N] are possible when the open-switch fault occurs in the $S_{x2}$ or $S_{x3}$ switch. Therefore, if the reference voltage is made using the voltage vector which does not contain the switching state [O] in a faulty leg, the distortion of the outputs is eliminated. For example, if $V_{\rm ref}$ falls into region 3 of sector II as shown in Fig. 14, the reference voltage $V_{\rm ref}$ is made using the nearest four switching states [OON], [OPN], [PPN], and [PPO], and the switching sequence is [OON]-[OPN]-[PPN]-[PPO]-[PPN]-[OPN]-[OON] in the normal condition.

If the open-switch fault occurs in switch $S_{a2}$ or $S_{a3}$, the switching state does not reach the desired state [OON] or [OPN] because the switching state [O] is impossible in a faulty leg A.

TABLE IV
PARAMETERS OF THE EXPERIMENTS

| Parameter | Value |
|---|---|
| DC-link voltage | *200 V* |
| Switching frequency | *10 kHz* |
| Control period | *100 μs* |
| Frequency of current | *60 Hz* |
| Load | *L: 10 mH, R: 10 Ω* |
| $I_{th}$, $V_{th}$ | *0.08, 10V* |

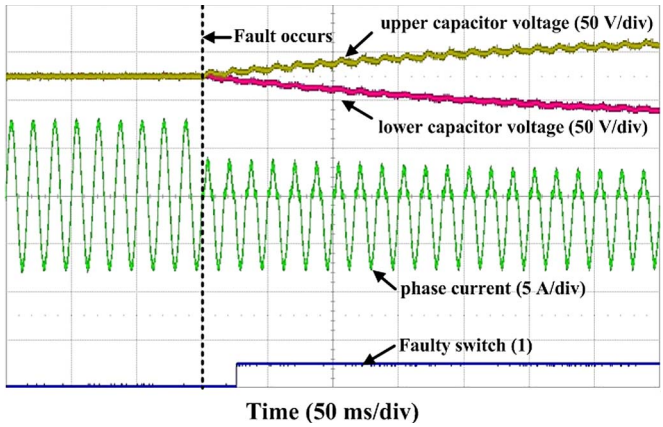


Fig. 26. Experimental results of proposed fault diagnosis method when the open-switch fault occurs in switch $S_{a1}$.

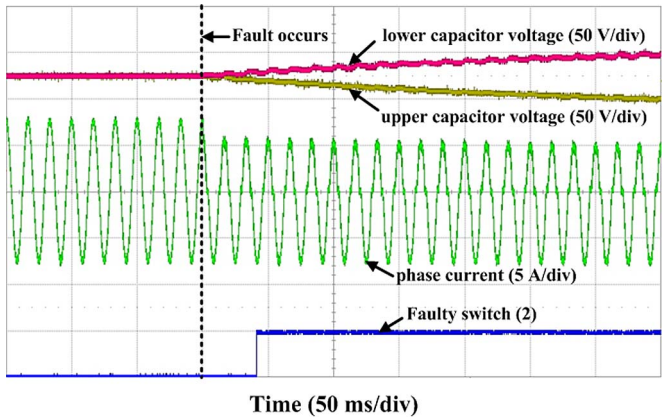


Fig. 27. Experiment results of proposed fault diagnosis method when the open-switch fault occurs in switch $S_{a2}$.

For such a reason as mentioned earlier, the phase current is distorted.

To eliminate the distortion, the [OON] and [OPN] should be replaced with the nearest switching state to themselves which excludes the [O] state in the faulty leg A. Thus, in this case, the switching states [OON] and [OPN] will be replaced with [NON] and [NPN], respectively. The new switching sequence is [NON]-[NPN]-[PPN]-[PPO]-[PPN]-[NPN]-[NON]. The proposed fault-tolerant control is very simple. In a conventional SVM approach, the positive-phase reference voltage is generated using switching states [P] and [O], and the negative-phase reference voltage is generated using switching states [O] and [N]. In the proposed method, if the open-switch fault occurs in switch $S_{x2}$ or $S_{x3}$, the reference voltage of the faulty leg is

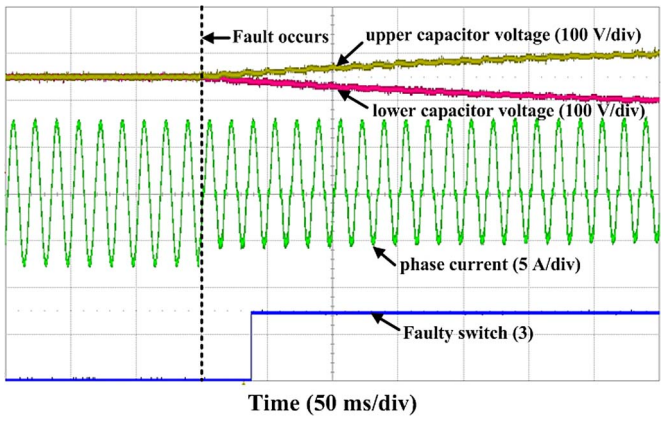


Fig. 28. Experiment results of proposed fault diagnosis method when the open-switch fault occurs in switch $S_{a3}$.

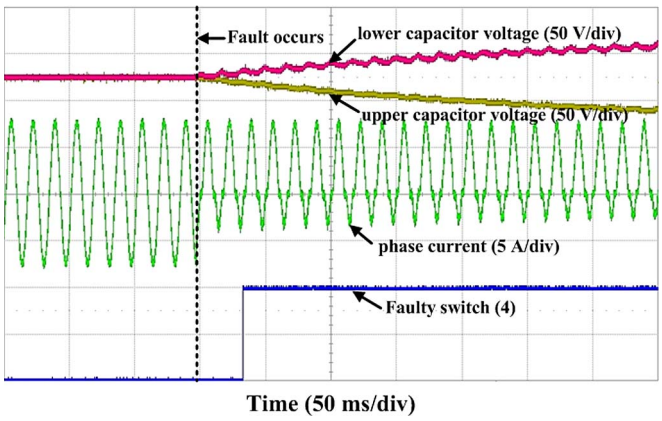


Fig. 29. Experiment results of proposed fault diagnosis method when the open-switch fault occurs in switch $S_{a4}$.

generated using [P] and [N]. This method is easily implemented by adding a time offset to the turn-on times of the faulty leg. The time offset is defined as follows:

$$T_{off} = -\frac{1}{2}T_x, \qquad \text{if } V_x^* > 0$$
$$T_{off} = -\frac{1}{2}T_x + \frac{1}{4}T_s, \qquad \text{if } V_x^* < 0 \tag{6}$$

where the $V_x^*$ is the reference voltage of the faulty leg and $T_s$ is the switching period.

Assuming that the open-switch fault occurs in leg A, the turn-on time $T_a$ is redefined as follows:

$$T_a^{'} = \frac{1}{2}T_a, \qquad \text{if } V_a^* > 0$$
$$T_a^{'} = \frac{1}{2}\left(T_a + \frac{1}{2}T_s\right), \qquad \text{if } V_a^* < 0. \tag{7}$$

The reference voltage of phase A is made by the gate-on time $T_a'$. The switches $S_{a1}$ and $S_{a2}$ are turned-on using the redefined turn-on time $T_a'$ simultaneously, and the switches $S_{a3}$ and $S_{a4}$ are operated complementary to $S_{a1}$ and $S_{a2}$. Fig. 15 shows the block diagram of the proposed strategy when the open-switch fault occurs in neutral switches.

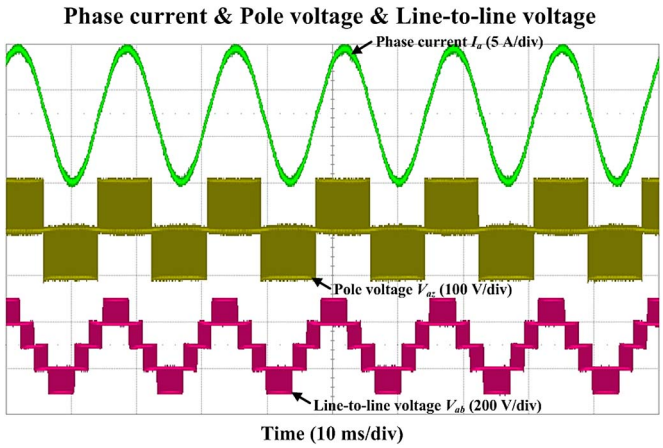


Fig. 30. Outputs of T-type three-level inverter under normal condition.

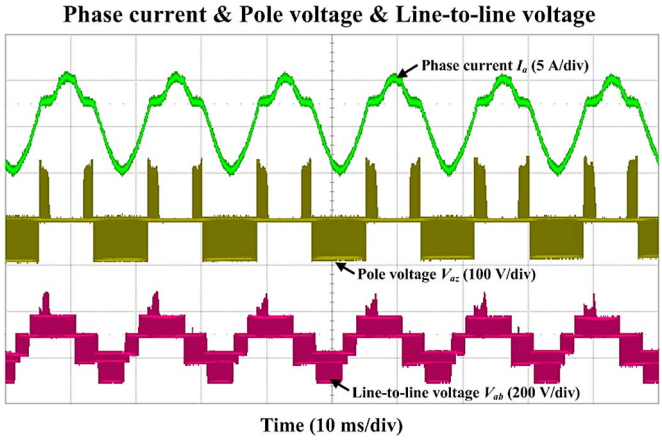


Fig. 31. Outputs of T-type three-level inverter under switch $S_{a1}$ fault condition.

## V. Simulation

Simulations have been carried out to verify the validity of the proposed algorithm. The simulation parameters are listed in Table III.

Fig. 16 shows the results of the proposed fault diagnosis method when the open-switch fault occurs in switch $S_{a1}$. In this case, the output phase currents are distorted as expressed and described in Section III. Therefore, the diagnosis variables $\mu_a$ has $-1$, and $\mu_b$ has $+1$ as shown in Fig. 16(b). Furthermore, the upper capacitor voltage $V_{\mathrm{DC1}}$ becomes larger than the lower capacitor voltage $V_{\mathrm{DC2}}$. Hence, the diagnosis variable $V_d$ has 1 as shown in Fig. 16(c). As shown in Table I, these values of diagnosis variables signify that the open-switch fault occurs in switch $S_{a1}$. The SW signal represents the faulty switch. As shown in Fig. 16(d), the faulty switch is identified correctly by the proposed method.

The waveforms given in Figs. 17–19 show the results of the proposed fault diagnosis method when the open-switch fault occurs in $S_{a2}$, $S_{a3}$, and $S_{a4}$, respectively. The diagnosis variables have accurate values as the previous analysis in all faulty cases in leg A. Using these variables, the faulty switches are identified correctly within 40 ms through the proposed method as shown in Figs. 17–19. The diagnosis time is dependent on the magnitude phase current and the threshold values.

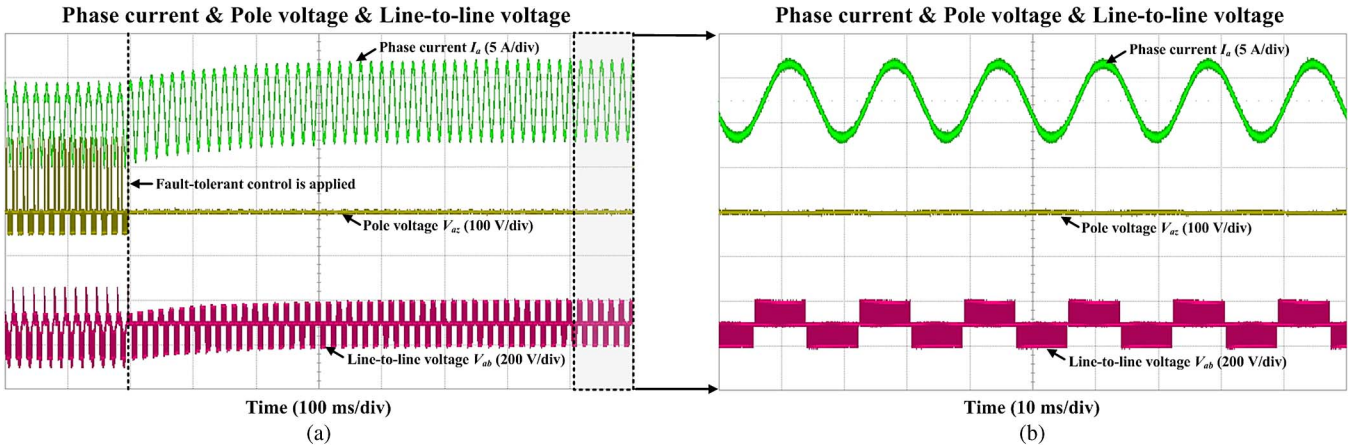


Fig. 32. Outputs of T-type three-level inverter when the proposed method is applied under switch $S_{a1}$ fault condition.

If the phase current is larger, the diagnosis time will be shortened because the two-capacitor voltages are changed more swiftly. If the threshold values are small, the diagnosis time can be reduced, but the accuracy can also be reduced. Therefore, the threshold values should be chosen properly.

Fig. 20 shows the simulation results of the proposed fault-tolerant strategy when the open-switch fault occurs in $S_{a1}$. The distortion of phase current is eliminated after the proposed algorithm is applied. The output line-to-line voltage is not five levels but three levels, and the magnitude of phase current is decreased because the modulation index is reduced for fault-tolerant control. After the proposed algorithm is applied, the output pole voltage of the A-phase is fixed to zero. It means that the switches $S_{a1}$ and $S_{a4}$ are not used in this method.

Fig. 21 shows the comparison results whether considering or not considering the steps 3 and 4 in Section III. As shown in Fig. 21(b), if steps 3 and 4 are not considered, the neutral-point voltage is unbalanced. If only step 4 is not applied, although the slope of the neutral-point voltage's change is smaller than the earlier case, the two capacitors have different values as shown in Fig. 21(c). It proves that the steps 3 and 4 should be considered to balance the neutral-point voltage when the fault-tolerant control is applied.

Fig. 22 shows the results of the proposed algorithm when the switch $S_{a2}$ is faulty. The phase current is distorted after the fault occurs. After the proposed control is applied, the phase currents are almost the same as those in normal operation. In this case, the reference voltage is made using the switching states [P] and [N] in the faulty leg. Therefore, the pole voltage is two levels.

Figs. 23 and 24 show the results of the proposed algorithm when the switches $S_{b3}$ and $S_{c4}$ are faulty, respectively. These results also prove that the proposed algorithm is useful when the open-switch fault occurs in the T-type three-level inverter.

## VI. Experimental Results

A prototype of the T-type three-level inverter systems was built to verify the proposed fault diagnosis method and fault-tolerant control strategy. Fig. 25 shows the prototype of the T-type three-level inverter systems. The digital controller is based on a digital signal processor (TMS320F28335), and

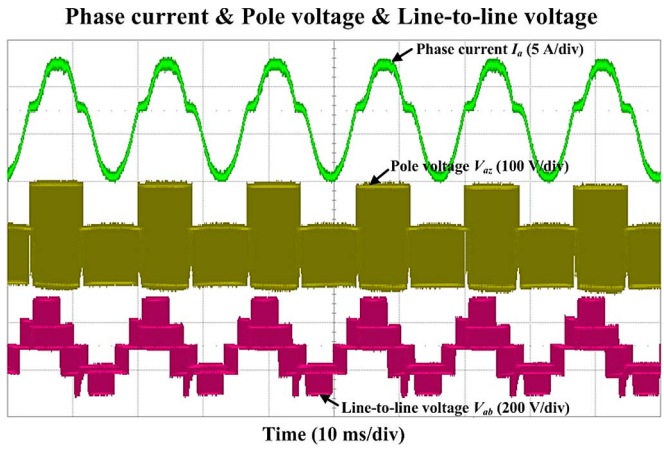


Fig. 33. Outputs of T-type three-level inverter under switch $S_{a2}$ fault condition.

1200-V 300-A Fuji IGBTs were used. The parameters of the experiments are shown in Table IV. In the experiments, the phase current is normalized by 20 A.

Fig. 26 shows the experimental results of the proposed fault diagnosis method when the open-switch fault occurs in switch $S_{a1}$. After the fault occurs, the phase current is distorted, and the upper capacitor voltage becomes larger than the lower capacitor voltage as discussed in the previous analysis. The faulty switch is detected within 30 ms.

Figs. 27–29 show the experimental results when the open-switch fault occurs in switch $S_{a2}$, $S_{a3}$, and $S_{a4}$, respectively. In all cases, the faulty switch is identified accurately in about 50 ms. More time is needed to detect the fault switch when the open-switch fault occurs in neutral-point switches ($S_{x2}$ or $S_{x3}$) than when the open-switch fault occurs in half-bridge switches ($S_{x1}$ or $S_{x4}$). This is because the phase currents are less distorted in the neutral-switch fault case than that of the half-bridge switch fault case. This diagnosis time is closely related to the magnitude of phase current, size of the capacitor, and threshold value. The experimental results prove that the proposed fault diagnosis method precisely detects the faulty switch.

Fig. 30 shows the phase current, output pole voltage, and line-to-line voltage of the T-type 3-level inverter under the

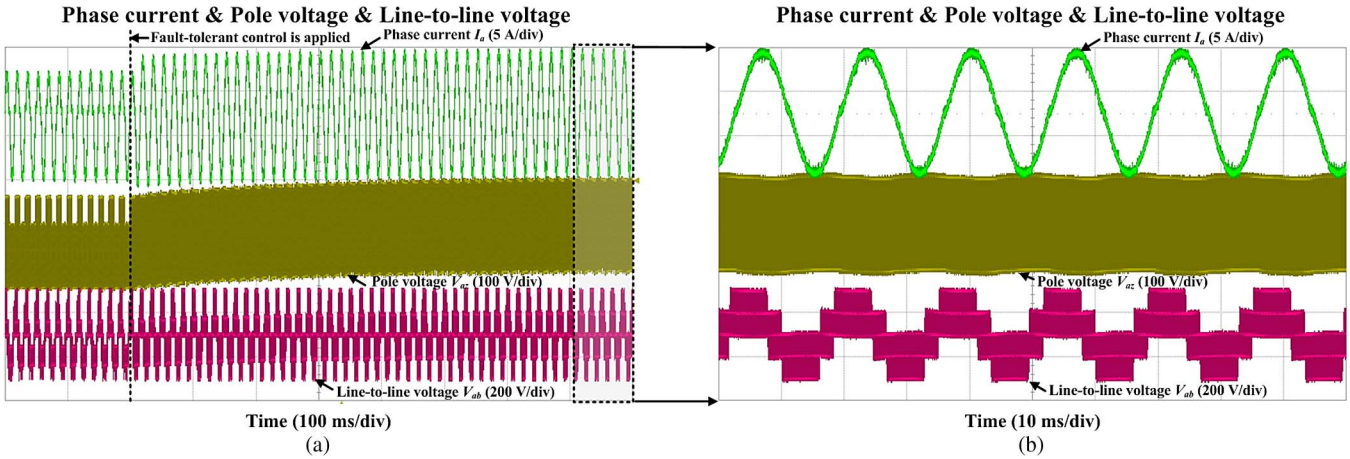


Fig. 34. Outputs of T-type three-level inverter when the proposed method is applied under switch $S_{a2}$ fault condition.

normal condition. If the open-switch fault occurs in switch $S_{a1}$, the undesirable output pole voltage is produced, and the phase current is distorted as shown in Fig. 31.

Fig. 32 shows the experimental results after the proposed fault-tolerant control is applied when the switch $S_{a1}$ is faulty. The output line-to-line voltage is not five levels but three levels, and the magnitude of the output phase current is decreased because the modulation index is reduced so that the $V_{\rm ref}$ is in the inner hexagon of the space vector diagram. In this control, the output pole voltage is fixed to zero. It means that the switches $S_{a1}$ and $S_{a4}$ are not used in this method. Therefore, the distortion due to the switching states [P] and [N] does not occur. Although the magnitude of output phase current is decreased, the distortion of the phase current is eliminated.

Figs. 33 and 34 show the phase current, output phase current, and line-to-line voltage when the open-switch fault occurs in switch $S_{a2}$ and the proposed control is applied, respectively. As the earlier study, if the open-switch fault occurs in switch $S_{a2}$, the output phase current is distorted due to the undesirable output pole voltage $-V_{\rm DC}/2$ instead of zero. After the proposed control is applied, the output pole voltage of the faulty phase becomes two levels, and the distortion of the phase current is eliminated because, in the proposed method, the switching state [O] in the faulty leg A is not used. In this case, the inverter is operated without a decrease of the phase current because the proposed fault-tolerant control can be applied without reducing the modulation index. The total harmonic distortion (THD) is increased a little bit compared to the THD under the normal condition since this method does not use the switching state [O] in the faulty leg. Nevertheless, the experimental results demonstrate that the T-type inverter is operated with the well-maintained performance by the proposed fault-tolerant control when a neutral switch fails.

## VII. Conclusion

This paper has analyzed the operation of the T-type three-level inverter under the open-switch fault condition and presented the diagnosis method of an open-switch fault and fault-tolerant control strategy for continuous operation. The faulty switch is precisely identified by the proposed methods. By the proposed fault-tolerant control strategies, the distortion of phase current disappeared, and the T-type inverter is continuously operated. In the half-bridge switch fault case, the distortion of phase current is eliminated, although the magnitude of phase currents is reduced. In this case, the modulation index should be reduced until the reference voltage is in the inner hexagon of the voltage diagram. Furthermore, the balance of the neutral-point voltage should be considered. In the neutral-switch fault case, the distortion of output phase currents is eliminated well without the decrease of phase currents. By the proposed methods, the applications using the T-type three-level systems such as servo drive systems, PV systems, and other small power applications have more reliability in regard to the open-switch fault. The proposed algorithms do not require additional hardware and complex calculations. Therefore, the methods are cost-effective and simple to implement. The simulation and experimental results confirm the feasibility of the proposed fault diagnosis and tolerant control strategy.

## References

[1] M. Schweizer and J. W. Kolar, "Design and implementation of a highly efficient 3-level T-type converter for low-voltage application," *IEEE Trans. Power Electron.*, vol. 28, no. 2, pp. 899–907, Feb. 2013.

[2] M. Schweizer, I. Lizama, T. Friedli, and J. W. Kolar, "Comparison of the chip area usage of 2-level and 3-level voltage source converter topologies," in *Conf. Rec. IEEE IECON*, 2010, pp. 391–396.

[3] K. Komatsu, M. Yatsu, S. Miyashita, S. Okita, H. Nakazawa, S. Igarashi, Y. Takahashi, Y. Okuma, Y. Seki, and T. Fujihira, "New IGBT modules for advanced neutral-point-clamped 3-level power converters," in *Conf. Rec. IPEC*, 2010, pp. 523–527.

[4] L. Ma, K. Sun, and X. Jin, "A transformation method from conventional three phase full-bridge topology to conergy NPC topology," in *Conf. Rec. ICEMS*, 2011, pp. 1–5.

[5] U. M. Choi, H. G. Jeong, K. B. Lee, and F. Blaabjerg, "Method for detecting an open-switch fault in a grid-connected NPC inverter system," *IEEE Trans. Power Electron.*, vol. 27, no. 6, pp. 2726–2739, Jun. 2012.

[6] T. J. Kim, W. C. Lee, and D. S. Hyun, "Detection method for open-circuit fault in neutral-point clamped inverter systems," *IEEE Trans. Ind. Electron.*, vol. 56, no. 7, pp. 2754–2763, Jul. 2009.

[7] S. Khomfoi and L. M. Tolbert, "Fault diagnostic system for a multilevel inverter using a neural network," *IEEE Trans. Power Electron.*, vol. 22, no. 3, pp. 1062–1069, May 2007.

[8] U. M. Choi, K. B. Lee, and F. Blaabjerg, "Diagnosis method of an open-switch fault for a grid-connected T-type three-level inverter system," in *Conf. Rec. PEDG*, 2012, pp. 470–475.

[9] U. M. Choi and K. B. Lee, "Detection method of an open-switch fault and fault-tolerant strategy for a grid-connected T-type three-level inverter system," in *Conf. Rec. ECCE*, 2012, pp. 4188–4195.

[10] B. Lu and S. K. Sharma, "A literature review of IGBT fault diagnostic and protection methods for power inverter," *IEEE Trans. Ind. Appl.*, vol. 45, no. 5, pp. 1770–1777, Sep./Oct. 2009.
[11] Y. J. Ko and K. B. Lee, "Fault diagnosis of a voltage-fed PWM inverter for a three-parallel power conversion system in a wind turbine," *J. Power Electron.*, vol. 10, no. 6, pp. 686–693, Nov. 2010.
[12] P. Lezana, J. Pou, T. A. Meynard, J. Rodriquez, S. Ceballos, and F. Richardequ, "Survey on fault operation on multilevel inverters," *IEEE Trans. Ind. Electron.*, vol. 57, no. 7, pp. 2207–2218, Jul. 2010.
[13] Y. J. Ko, K. B. Lee, D. C. Lee, and J. M. Kim, "Fault diagnosis of three-parallel voltage-source converter for a high-power wind turbine," *IET Power Electron.*, vol. 5, no. 7, pp. 1058–1067, Aug. 2012.
[14] S. Ceballos, J. Pou, E. Robles, J. Zaragoza, and J. L. Martin, "Performance evaluation of fault-tolerant neutral-point clamped converters," *IEEE Trans. Ind. Electron.*, vol. 57, no. 8, pp. 2709–2718, Aug. 2010.
[15] S. Ceballos, J. Pou, E. Robles, J. Zaragoza, E. Robles, J. L. Villate, and J. L. Martin, "Fault-tolerant neutral-point clamped converter solutions based on including a fourth resonant leg," *IEEE Trans. Ind. Electron.*, vol. 58, no. 6, pp. 2293–2303, Jun. 2011.
[16] X. Kou, K. A. Corzine, and Y. L. Familiant, "A unique fault-tolerant design for flying capacitor multilevel inverter," *IEEE Trans. Power Electron.*, vol. 19, no. 4, pp. 979–987, Jul. 2004.
[17] W. Song and A. Q. Huang, "Fault-tolerant design and control strategy for cascaded H-bridge multilevel inverter-based STATCOM," *IEEE Trans. Ind. Electron.*, vol. 57, no. 8, pp. 2700–2708, Aug. 2010.
[18] L. Maharjan, T. Yamagishi, H. Akagi, and J. Asakura, "Fault-tolerant operation of a battery-energy-storage system based on a multilevel cascade PWM converter with star configuration," *IEEE Trans. Power Electron.*, vol. 25, no. 9, pp. 2386–2396, Sep. 2010.
[19] U. M. Choi and K. B. Lee, "Neutral-point voltage balancing method for three-level inverter systems with a time-offset estimation scheme," *J. Power Electron.*, vol. 13, no. 2, pp. 243–249, Mar. 2013.
[20] U. M. Choi, H. H. Lee, and K. B. Lee, "Simple neutral-point voltage for three-level inverters using a discontinuous pulse width modulation," *IEEE Trans. Energy Convers.*, vol. 28, no. 2, pp. 434–443, Jun. 2013.
[21] U. M. Choi and K. B. Lee, "Space vector modulation strategy for neutral-point voltage balancing in three-level inverter systems," *IET Power Electron.*, vol. 6, no. 7, pp. 1390–1398, Aug. 2013.

**Ui-Min Choi** (S'11) was born in Icheon, Korea, in 1986. He received the B.S. and M.S. degrees in electrical and computer engineering from Ajou University, Suwon, Korea, in 2011 and 2013, respectively. He is currently working toward the Ph.D. degree at Aalborg University, Aalborg East, Denmark.

His research interests include power conversion, renewable power generation, multilevel converters, and reliability.

**Kyo-Beum Lee** (S'02–M'04–SM'11) received the B.S. and M.S. degrees in electrical and electronic engineering from Ajou University, Suwon, Korea, in 1997 and 1999, respectively, and the Ph.D. degree in electrical engineering from Korea University, Seoul, in 2003.

From 2003 to 2006, he was with the Institute of Energy Technology, Aalborg University, Aalborg East, Denmark. From 2006 to 2007, he was with the Division of Electronics and Information Engineering, Chonbuk National University, Jeonju, Korea. In 2007, he joined the School of Electrical and Computer Engineering, Ajou University. He is an Associate Editor of the *Journal of Power Electronics*. His research interests include electric machine drives and renewable power generations.

Dr. Lee is an Associate Editor of the IEEE TRANSACTIONS ON POWER ELECTRONICS and the IEEE TRANSACTIONS ON INDUSTRIAL ELECTRONICS.

**Frede Blaabjerg** (S'86–M'88–SM'97–F'03) received the Ph.D. degree from Aalborg University, Aalborg East, Denmark, in 1995.

From 1987 to 1988, he was with ABB-Scandia, Randers, Denmark. He is currently with the Department of Energy Technology, Aalborg University, where he became an Assistant Professor in 1992; an Associate Professor in 1996; a Full Professor in power electronics and drives in 1998; and was the Dean of the Faculty of Engineering, Science, and Medicine in 2006–2010. He was a Part-Time Research Leader in wind turbines with the Research Center Risoe. In 2009, he was a Visiting Professor with Zhejiang University, China. His research areas are in power electronics and applications, such as wind turbines, photovoltaic systems, and adjustable-speed drives.

Dr. Blaabjerg was a recipient of the 1995 Angelos Award for his contributions to modulation technique and the Annual Teacher Prize from Aalborg University. In 1998, he was a recipient of the Outstanding Young Power Electronics Engineer Award from the IEEE Power Electronics Society. He was a recipient of ten IEEE prize paper awards and another prize paper award at the International Conference on Power Electronics and Intelligent Control for Energy Conversation (PELINCEC 2005) in Poland. He was a recipient of the IEEE PELS Distinguished Service Award in 2009 and the 14th International Power Electronics and Motion Control Conference (EPE-PEMC 2010) Council Award. He was an Editor-in-Chief of the IEEE TRANSACTIONS ON POWER ELECTRONICS from 2006 to 2012. He was a Distinguished Lecturer of the IEEE Power Electronics Society from 2005 to 2007 and the IEEE Industry Applications Society from 2010 to 2011.